Why Does the Rhodium-Catalyzed Hydrosilylation of Alkenes Take Place through a Modified Chalk−Harrod Mechanism? A Theoretical Study

Shigeyoshi Sakaki,*,[†] Michinori Sumimoto,[‡] Mari Fukuhara,[§] Manabu Sugimoto,[‡]
Hitoshi Fujimoto,[‡] and Susumu Matsuzaki[‡]

Institute for Fundamental Research of Organic Chemistry, Kyushu University, Higashi-ku, Fukuoka 820-8581, Japan, Graduate School for Science and Technology, Kumamoto University, Kurokami, Kumamoto 860-8555, Japan, and Department of Applied Chemistry and Biochemistry, Faculty of Engineering, Kumamoto University, Kurokami, Kumamoto 860-8555, Japan

Received March 28, 2002

Rh-catalyzed hydrosilylation of ethylene was theoretically investigated with the DFT, MP4(SDQ), and CCSD(T) methods, where $RhCl(PH_3)_3$ was adopted as a model catalyst. The rate-determining step in the Chalk−Harrod mechanism is Si−C reductive elimination, the activation barrier (E_a) of which is 27.4 (28.8) kcal/mol, where the values without parenthesis and in parenthesis are calculated with the DFT and MP4(SDQ) methods, respectively. The rate-determining step in the modified Chalk−Harrod mechanism is either ethylene insertion into the $Rh-SiMe_3$ bond (E_a = 13.5 (16.9) kcal/mol) at the MP4(SDQ) level or oxidative addition of $HSiMe_3$ (E_a =15.7 (11.3) kcal/mol) at the DFT level. From these results, it should be clearly concluded that the Rh-catalyzed hydrosilylation of ethylene proceeds through the modified Chalk−Harrod mechanism, unlike Pt-catalyzed hydrosilylation of alkene, which takes place through the Chalk−Harrod mechanism. The difference between Rh and Pt catalysts arises from the facts that ethylene is more easily inserted into the $Rh-SiMe_3$ bond with a moderate E_a value than that into the $Pt-SiR_3$ bond (E_a = 41−60 kcal/mol) and the Si−C reductive elimination of $RhCl(CH_3)(SiMe_3)(PH_3)_2(C_2H_4)$ needs a very large E_a value. This difference in the ethylene insertion between Pt and Rh catalysts is reasonably interpreted in terms that an alkyl group is formed at a position trans to hydride in the Pt catalyst but formed at a position trans to PH_3 in the Rh catalyst. This is because ethylene can take a position trans to PH_3 in the pseudo-octahedral six-coordinate Rh(III) complex, but ethylene must take a position trans to hydride in the four-coordinate planar Pt(II) complex (remember that Rh(III) and Pt(II) have d^6 and d^8 electron configurations, respectively). The large E_a value of the Si−C reductive elimination results from the fact that both sp^3 valence orbitals of $SiMe_3$ and CH_3 must change their directions from the Rh center toward CH_3 and $SiMe_3$, respectively, in the transition state. The present theoretical calculations also show that β-H abstraction by the Rh center easily occurs in $RhClH(CH_2CH_2SiMe_3)(PH_3)_2$ to yield a Rh(III) vinylsilane complex, $\overline{RhCl(H)_2(CH_2}{=}CHSiMe_3)(PH_3)_2$, with a low activation barrier.

Introduction

Hydrosilylation of alkene is one of the important and versatile synthetic reactions of organic silicon compounds.[1] Speier's catalyst, which is chloroplatinic acid in ethanol,[2] is well-known because of its high catalytic activity, and the Chalk−Harrod mechanism was proposed first for Pt-catalyzed hydrosilylation of alkene.[1b,c,d,3] In this mechanism, alkene is inserted into a Pt−H bond followed by Si−C reductive elimination, to release a product (Scheme 1). Later, a modified Chalk−Harrod mechanism was proposed in Rh-, Co-, Fe-, and Ir-catalyzed hydrosilylations of alkene and alkyne.[1d,4−10] In this mechanism, alkene and alkyne are inserted into the $M-SiR_3$ bond followed by C−H reductive elimination (Scheme 1). If β-H abstraction occurs after alkene

---

* To whom correspondence should be addressed. E-mail: sakaki@mee3.moleng.Kyoto-u.ac.jp. Present address: Department of Molecular Engineering, Graduate School of Engineering, Kyoto University, Kyoto 606-8501, Japan.

[†] Kyushu University.

[‡] Graduate School for Science and Technology, Kumamoto University.

[§] Department of Applied Chemistry and Biochemistry, Faculty of Engineering, Kumamoto Univeristy.

(1) For instance: (a) Speier, J. L. *Adv. Organomet. Chem.* **1979**, *17*, 407. (b) Harrod, J. F.; Chalk, A. J. In *Organic Synthesis via Metal Carbonyls*; Wender, I., Pino, P., Eds.; John Wiley & Sons Ltd.: New York, 1977; Vol. 2, p 673. (c) Tilley, T. D. In *The Chemistry of Organic Silicon Compounds*; Patai, S., Rappoport, Z., Eds.; John Wiley & Sons Ltd.: New York, 1989; p 1415. (d) Ojima, I. In *The Chemistry of Organic Silicon Compounds*; Patai, S., Rappoport, Z., Eds.; John Wiley & Sons Ltd.: New York, 1989; p 1479. (e) Ohsima, K. In *Advances in Metal-Organic Chemistry*; Liebeskind, L. S., Ed.; JAI Press Ltd.: London, 1991; Vol. 2, p 101.

(2) (a) Speier, J. L.; Webster, J. A.; Barnes, G. H. *J. Am. Chem. Soc.* **1957**, *79*, 974. (b) Saam, J. C.; Speier, J. L. *J. Am. Chem. Soc.* **1958**, *80*, 4104. (c) Ryan, J. W.; Speier, J. L. *J. Am. Chem. Soc.* **1964**, *86*, 895.

10.1021/om020239j CCC: $22.00
Publication on Web 08/07/2002

Scheme 1

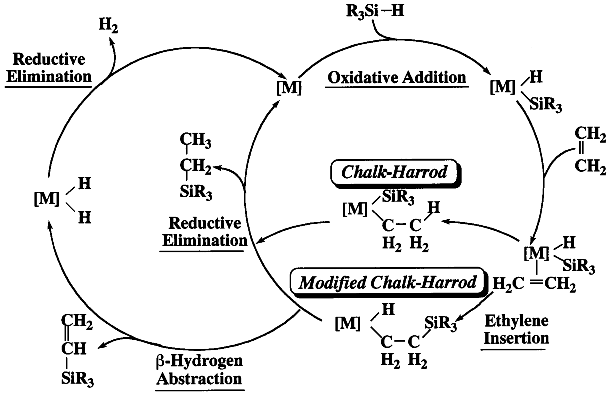

insertion into the M−SiR$_3$ bond, vinylsilane is produced, whereas vinylsilane cannot be produced at all in the Chalk−Harrod mechanism. Thus, formation of vinylsilane in Rh-catalyzed hydrosilylation of alkene is believed to be evidence of the modified Chalk−Harrod mechanism.[4,6−8,10] However, we do not know the reason that Rh-, Co-, Fe-, and Ir-catalyzed hydrosilylations proceed through the modified Chalk−Harrod mechanism unlike the Pt-catalyzed hydrosilylation. Moreover, we must take account of the possibility that formation of vinylsilane is not evidence of the modified Chalk−Harrod mechanism; that is, vinylsilane is formed through the alkene insertion into the M−SiR$_3$ bond followed by the β-H abstraction, but the hydrosilyaltion proceeds through the Chalk−Harrod mechanism. A similar proposal was experimentally presented.[11] Thus, it is considerably important and interesting to investigate theoretically whether the hydrosilylation occurs through the modified Chalk−Harrod mechanism when Rh, Co, Fe, and Ir complexes are used as a catalyst.

Previously, Gordon and his collaborators theoretically investigated Ti-catalyzed hydrosilyaltion of ethylene and reported that the reaction proceeds with a very small activation barrier.[12] Also, we theoretically investigated Pt-catalyzed hydrosilyaltion of ethylene and clearly concluded that this reaction takes place through the Chalk−Harrod mechanism.[13] However, no theoretical investigation has presented any evidence that supports the modified Chalk−Harrod mechanism.

In this work, we theoretically investigated Rh-catalyzed hydrosilylation of ethylene with the DFT, MP4(SDQ), and CCSD(T) methods. Our purposes here are to investigate theoretically if the Rh-catalyzed hydrosilylation of ethylene occurs through the modified Chalk−Harrod mechanism, to clarify the reasons that the modified Chalk−Harrod mechanism is more favorable than the Chalk−Harrod mechanism in the Rh-catalyzed hydrosilylation unlike the Pt-catalyzed hydrosilylation, and to show clear differences in the hydrosilylation reaction between Rh and Pt catalysts.

Computational Details

Geometry optimization was carried out with the DFT method,[14−16] where the B3LYP functional was adopted for the exchange−correlation term. In the geometry optimization, the following basis set system (BS-I) was used: core electrons of Rh (up to 3d), P, Si, and Cl (up to 2p) were replaced with effective core potentials (ECPs),[17] and their valence electrons were represented with split valence type basis sets, (311/311/31)[17] for Rh and (21/21)[17] for the other elements, respectively. A d-polarization function was added to Si.[18] The MIDI-3 basis set[19] was employed for C, where a d-polarization function was added to C except for C of SiMe$_3$. Energy changes were evaluated with the DFT and MP4(SDQ) methods, using a better basis set system (BS-II), where the DFT/BS-I optimized geometries were adopted. In BS-II, valence electrons of Rh were represented by a (541/541/111) set[20] with the same ECPs as those of BS-I. Huzinaga−Dunning (9s5p1d)/[3s2p1d] and (13s8p1d)/[6s4p1d] sets were used for C and Si,[21] respectively, while a d-polarization function was not added to C of SiMe$_3$. For Cl and P, the same basis sets and the same ECPs as those of BS-I were used.

Important transition states and intermediates that are involved in the most favorable reaction course in the Chalk−Harrod and modified Chalk−Harrod mechanisms were ascertained by vibrational frequency calculations with the DFT/BS-I method.

When the DFT and MP4(SDQ) methods yielded a considerably different value of energy change, we calculated the energy change with the CCSD(T) method. In these MP4(SDQ) and CCSD(T) calculations, core orbitals were excluded from the active space. In the CCSD(T) calculations, contribution of triple substitutions was incorporated noniteratively with single and double substitution wavefunctions.[22] All these calculations were carried out with the Gaussian 98 program package.[23]

RhCl(PH$_3$)$_3$ and HSiMe$_3$ were adopted here as model catalyst and hydrosilane, respectively, since Rh(I) complexes including Wilkinson's complex[1b,d,7,8b,24,25] and such hydrosilanes as trialkylhydrosilane, trichlorohydrosilane, and dialkylphenylhydrosilane were experimentally used.[7,8b]

---

(3) Chalk, A. J.; Harrod, J. F. *J. Am. Chem. Soc.* **1965**, *87*, 16.

(4) (a) Schroeder, M. A.; Wrighton, M. S. *J. Organomet. Chem.* **1977**, *128*, 345. (b) Reichel, C. L.; Wrighton, M. S. *Inorg. Chem.* **1980**, *19*, 3858. (c) Randolph, C. L.; Wrighton, M. S. *J. Am. Chem. Soc.* **1986**, *108*, 3366. (d) Seitz, F.; Wrighton, M. S. *Angew. Chem., Int. Ed. Engl.* **1988**, *27*, 289.

(5) Oro, L. A.; Fernandez, M. J.; Esteruelas, M. A.; Jimenez, M. S. *J. Mol. Catal.* **1986**, *37*, 151.

(6) (a) Milan, A.; Towns, E.; Maitlis, P. M. *J. Chem. Soc., Chem. Commun.* **1981**, 673. (b) Milan, A.; Fernandez, M.-J.; Bentz, P.; Maitlis, P. M. *J. Mol. Catal.* **1984**, *26*, 89.

(7) (a) Onopchenko, A.; Sabourin, E. T.; Beach, D. L. *J. Org. Chem.* **1983**, *48*, 5101. (b) Onopchenko, A.: Sabourin, E. T.; Beach, D. L. *J. Org. Chem.* **1984**, *49*, 3389. (c) Onopchenko, A.: Sabourin, E. T. *J. Org. Chem.* **1987**, *52*, 4118.

(8) (a) Ojima, I.; Yatabe, M.; Fuchikami, T. *J. Organomet. Chem.* **1984**, *260*, 335. (b) Ojima, I.; Clos, N.; Donovan, R. J.; Ingallina, P. *Organometallics* **1990**, *9*, 3127.

(9) Bergens, S. H.; Noheda, P.; Whelan, J.; Bosnich, B. *J. Am. Chem. Soc.* **1992**, *114*, 2128.

(10) Duckett, S. B.; Perutz, R. N. *Organometallics* **1992**, *11*, 90.

(11) Hostetler, M. J.; Butts, M. D.; Bergman, R. G. *Organometallics* **1993**, *12*, 65.

(12) Bode, B. M.; Day, P. N.; Gordon, M. S. *J. Am. Chem. Soc.* **1998**, *120*, 1552.

(13) (a) Sakaki, S.; Mizoe, N.; Sugimoto, M. *Organometallics* **1998**, *17*, 2510. (b) Sakaki, S.; Mizoe, N.; Musashi, Y.; Sugimoto, M. *J. Mol. Struct. (THEOCHEM)* **1999**, *461−462*, 533. (c) Sakaki, S.; Mizoe, N.; Sugimoto, M.; Mushashi, Y. *Coord. Chem. Rev.* **1999**, *190−192*, 933.

(14) (a) Becke, A. D. *Phys. Rev.* **1988**, *A38*, 3098. (b) Becke, A. D. *J. Chem. Phys.* **1993**, *98*, 1372, 5648.

(15) Lee, C.; Yang, W.; Parr, R. G. *Phys. Rev.* **1988**, *B37*, 785.

(16) Vosko, S. H.; Wilk, L.; Nusair, M. *Can. J. Chem.* **1980**, *58*, 1200.

(17) (a) Hay, P. J.; Wadt, W. R. *J. Chem. Phys.* **1985**, *82*, 299. (b) Wadt, W. R.; Hay, P. J. *J. Chem. Phys.* **1985**, *82*, 284.

(18) Hollwarth, A.; Bohme, M.; Dapprich, S.; Ehlers, A. W.; Gobbi, A.; Jonas, V.; Kohler, K. F.; Stegmann, R.; Veldkamp, A.; Frenking, G. *Chem. Phys. Lett.* **1993**, *208*, 237.

(19) Huzinaga, S.; Andzelm, J.; Klobukowski, M.; Radzio-Andzelm, E.; Sakai, Y.; Tatewaki, H. *Gaussian Basis Sets for Molecular Calculations*; Elsevier: Amsterdam, 1984.

(20) Couty, M.; Hall, M. B. *Chem. Phys. Lett.* **1996**, *17*, 1359.

(21) Dunning, T. H.; Hay, P. J. In *Methods of Electronic Structure Theory*; Schaeffer, H. F., Ed.; Plenum: New York, 1977, p 1.

(22) Pople, J. A.; Head-Gordon, M.; Raghavachari, K. *J. Chem. Phys.* **1987**, *87*, 5968.

Scheme 2

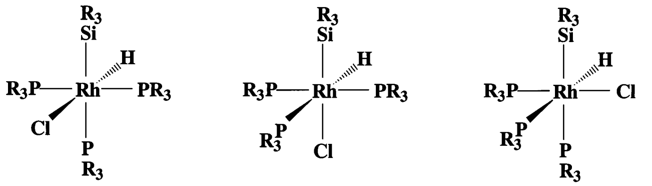

2a **2b** **2c**

Results and Discussion

Oxidative Addition of H−SiMe$_3$ to RhCl(PH$_3$)$_3$. The Si−H oxidative addition of HSiR$_3$ to RhCl(PH$_3$)$_3$ (**1**) yields RhClH(SiR$_3$)(PH$_3$)$_3$, in which we take three isomers (**2a**−**2c**) into consideration, as shown in Scheme 2. In **2a**, two PH$_3$ ligands take positions trans to each other and Cl takes a position trans to H(hydride). In **2b**, Cl is at a position trans to SiR$_3$, and two PH$_3$ ligands take positions trans to each other like those of **2a**. In **2c**, two PH$_3$ ligands take positions trans to H and SiR$_3$. Apart from **2a**, **2b**, and **2c**, there is the other isomer in which the H(hydride) ligand is at a position trans to SiMe$_3$. However, this isomer cannot be produced directly by oxidative addition of HSiMe$_3$ to RhCl(PH$_3$)$_3$. Although there is the possibility that Cl dissociation from the Rh(I) center followed by isomerization leads to this isomer, the Cl dissociation does not easily occur in solvents such as benzene and toluene which were experimentally used.[7,8] Thus, we excluded this isomer from the present investigation. Relative stabilities of **2a**, **2b**, and **2c** were investigated first. When PH$_3$ and SiMe$_3$ are adopted as models of phosphine and silyl ligands, respectively, **2c** is slightly less stable than **2a** and **2b** by only 0.2 and 0.8 kcal/mol (DFT/BS-I), respectively. However, when PMe$_3$ and SiH$_3$ are adopted as models of phosphine and silyl ligands, respectively, **2c** is considerably less stable than **2a** and **2b** by 7.0 and 18.3 kcal/mol, respectively.[26] This is because PMe$_3$, which has a stronger trans influence than that of PH$_3$, takes positions trans to H and SiMe$_3$. Similar results were theoretically discussed in the oxidative addition of H$_2$ to IrCl(CO)(PH$_3$)$_2$.[27] Hence, we examined here the oxidative addition reactions leading to **2a** and **2b**.

Geometry changes of these oxidative additions are shown in Figure 1. Here, we make a brief comparison in the bond distance of **1** between the experimental value and the computational one; the calculated Rh−P distance is in the range of experimental values (2.361−2.297 Å) of similar Rh(I) complexes,[28] and the Rh−Cl distance is slightly longer than the experimental one (2.321−2.365 Å).[28] These results indicate that the computational method employed here provides reasonable geometry. In the precursor complexes (**PC1** and **PC2**), HSiMe$_3$ is more distant from Rh, and both HSiMe$_3$ and RhCl(PH$_3$)$_3$ moieties do not distort much. These geometrical features are essentially the same as those of the precursor complex in the Si−H oxidative addition to Pt(PH$_3$)$_2$.[13,29] In transition states ($\mathbf{TS_{1-2a}}$ and $\mathbf{TS_{1-2b}}$), the Si−H bond lengthens to 1.598 and 1.574 Å, respectively. These distances are somewhat longer than that of the transition state in the Si−H oxidative addition to Pt(PH$_3$)$_2$.[13,28] The Cl−Rh−PH$_3$ angle considerably decreases to about 120° in the transition state of the Rh reaction system, while the P−Pt−P angle moderately decreases to 166° in the transition state of the Pt reaction system. These features indicate that $\mathbf{TS_{1-2a}}$ and $\mathbf{TS_{1-2b}}$ are less reactant-like than the transition state of the Pt reaction system.

In **2a**, the Rh−PH$_3$ bond at a position trans to SiMe$_3$ is considerably longer than the other Rh−PH$_3$ bonds (see Figure 1). Similarly in **2b**, the Rh−PH$_3$ bond at a position trans to H(hydride) is the longest, while the Rh−PH$_3$ bond at a position trans to PH$_3$ is the shortest. These results clearly indicate that the trans influence becomes stronger in the order PH$_3$ < H(hydride) < SiMe$_3$. Similar results were theoretically reported in *cis*-PtH(SiR$_3$)(PH$_3$)$_2$.[13,29] Complex **2b** is slightly more stable than **2a** by only 0.7 kcal/mol (DFT/BS-II).

Binding energy (BE), activation barrier (E_a), and reaction energy (ΔE) are listed in Table 1, where the binding energy is defined as the energy difference between the precursor complex and the sum of reactants, the activation energy is the energy difference between the transition state and the precursor complex, and the reaction energy is the energy difference between the product and the sum of reactants. A negative value of ΔE represents that the reaction is exothermic. First, we will compare BE, E_a, and ΔE values of the oxidative addition **1** → **2a** between the DFT and MP4(SDQ) methods. As shown in Table 1, the DFT method yields a smaller BE value than the MP4(SDQ) method. This is probably because the DFT method does not efficiently incorporate the dispersion interaction, which is important in this kind of complex. Also, the E_a value (15.7 kcal/mol) evaluated with the DFT method is considerably larger than that (11.3 kcal/mol) evaluated with the MP4(SDQ) method, and the exothermicity (8 kcal/mol) evaluated with the DFT method is much smaller than that (24.3 kcal/mol) evaluated with the MP4(SDQ) method. Since these two methods provide considerably different E_a and ΔE values, we calculated the E_a value with the CCSD(T) method. The E_a value moderately fluctuates around the MP2 and MP3 levels but fluctuates little upon going from MP4(DQ) to CCSD(T). From these results, it is reasonably concluded that the MP4-

---

(23) Frisch, M. J.; Trucks, G. W.; Schlegel, H. B.; Scuseria, G. E.; Robb, M. A.; Cheeseman, J. R.; Zakrzewski, V. G.; Montgomery, J. A., Jr.; Stratmann, R. E.; Burant, J. C.; Dapprich, S.; Millam, J. M.; Daniels, A. D.; Kudin, K. N.; Strain, M. C.; Farkas, O.; Tomasi, J.; Barone, V.; Cossi, M.; Cammi, R.; Mennucci, B.; Pomelli, C.; Adamo, C.; Clifford, S.; Ochterski, J.; Petersson, G. A.; Ayala, P. Y.; Cui, Q.; Morokuma, K.; Malick, D. K.; Rabuck, A. D.; Raghavachari, K.; Foresman, J. B.; Cioslowski, J.; Ortiz, J. V.; Stefanov, B. B.; Liu, G.; Liashenko, A.; Piskorz, P.; Komaromi, I.; Gomperts, R.; Martin, R. L.; Fox, D. J.; Keith, T.; Al-Laham, M. A.; Peng, C. Y.; Nanayakkara, A.; Gonzalez, C.; Challacombe, M.; Gill, P. M. W.; Johnson, B. G.; Chen, W.; Wong, M. W.; Andres, J. L.; Head-Gordon, M.; Replogle, E. S.; Pople, J. A. *Gaussian 98*, Gaussian, Inc.: Pittsburgh, PA, 1998.

(24) (a) Osborn, J. A.; Jardine, F. M.; Young, J. F.; Wilkinson, G. *J. Chem. Soc. A* **1966**, 1711. (b) Osborn, J. A.; de Charentenay, F.; Wilkinson, G. *J. Chem. Soc. A* **1968**, 789.

(25) (a) Duczmai, W.; Urbaniak, W.; Marciniec, B. *J. Organomet. Chem.* **1986**, *317*, 85. (b) Duczmai, W.; Urbaniak, W.; Marciniec, B. *J. Organomet. Chem.* **1987**, *327*, 295.

(26) The MP4(SDQ)/BS-II//HF/BS-I method was employed in the preliminary calculations.

(27) Sargent, A. L.; Hall, M. B. *Inorg. Chem.* **1992**, *31*, 317.

(28) (a) Busetto, C.; D'Alfonso, A.; Maspero, F.; Perego, G. *J. Chem. Soc., Dalton Trans.* **1977**, 1828. (b) Thorn, D. L.; Tulip, T. H.; Ibers, J. A. *J. Chem. Soc., Dalton Trans.* **1979**, 2022.

(29) Sakaki, S.; Mizoe, N.; Musashi, Y.; Biswas, B.; Sugimoto, M. *J. Phys. Chem.* **1998**, *102*, 8027.

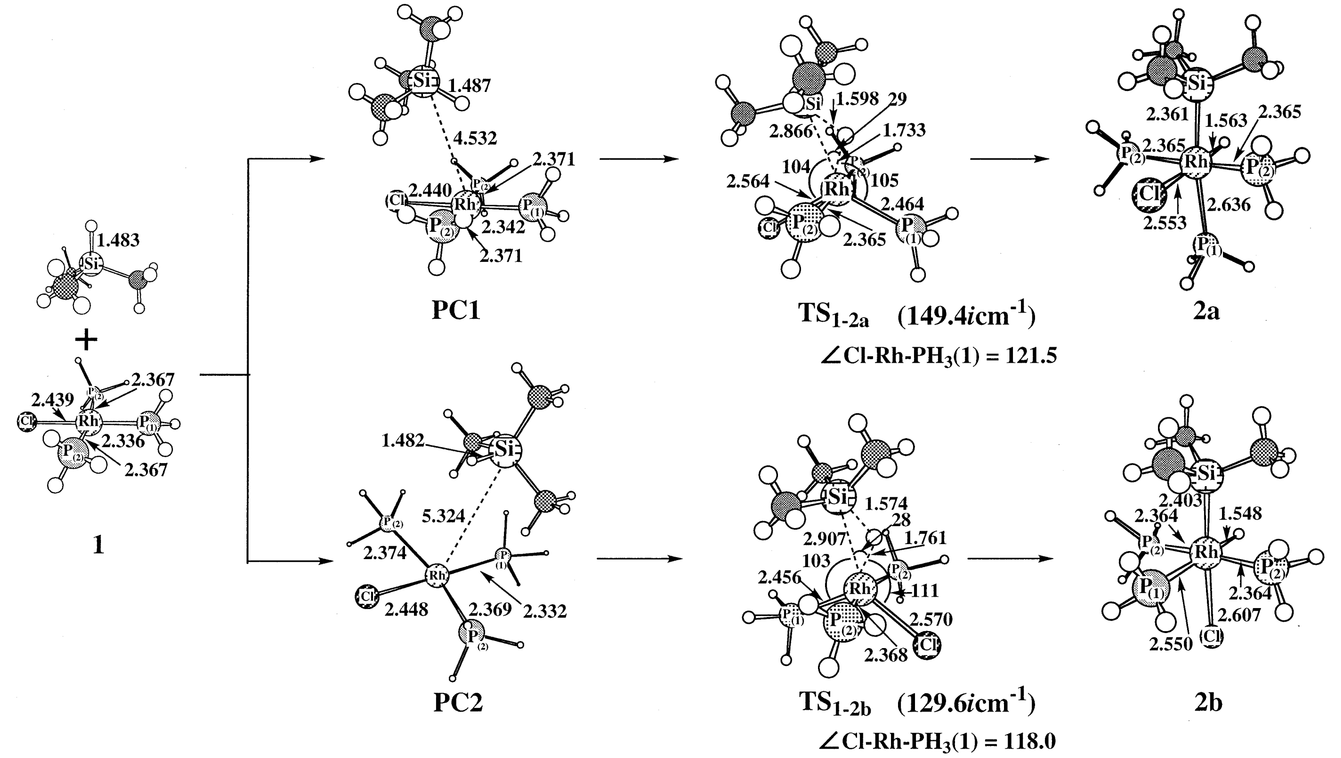

Figure 1. DFT-optimized geometry changes in the Si−H oxidative addition of $HSiMe_3$ to $RhCl(PH_3)_3$. Bond lengths in Å and bond angles in deg.

Table 1. Binding Energy (BE),[a] Activation Barrier (E_a),[b] and Reaction Energy (ΔE)[c] of the Oxidative Addition of $HSiMe_3$ to $RhCl(PH_3)_3$ (kcal/mol unit)

	BE	E_a	ΔE
	1 → **2a**		
DFT	−3.0	15.7	−8.0
MP2	−5.8	10.7	−31.9
MP3	−6.1	14.7	−17.1
MP4(DQ)	−5.6	13.1	−24.3
MP4(SDQ)	−5.7	11.3	−24.3
CCSD(T)		11.2	
	1 → **2b**		
DFT	−3.0	17.3	−8.7
MP4(SDQ)	−5.7	13.3	−26.3

[a] The stabilization energy of the precursor complexes relative to the sum of reactants, where a negative value represents the stabilization energy. [b] The energy difference between the transition state and the precursor complex. [c] The energy difference between the product and the sum of reactants.

(SDQ) and CCSD(T) methods seem reliable in the oxidative addition.

Now, let us make a comparison between two oxidative additions **1** → **2a** and **1** → **2b**. The binding energies (BE) of **PC1** and **PC2** are very small, which is consistent with our understanding that **PC1** and **PC2** are van der Waals complexes. Apparently, the oxidative addition **1** → **2b** occurs with a somewhat smaller E_a value and slightly larger exothermicity than does the reaction **1** → **2a**, as shown in Table 1. This is probably because Cl, the trans influence of which is weaker than that of PH_3, takes a position trans to $SiMe_3$ in **2b**.

It should be noted here that the oxidative addition of $HSiMe_3$ to **1** occurs with a much larger E_a value than that to $Pt(PH_3)_2$.[13] To clarify the reason for the difference between $RhCl(PH_3)_3$ and $Pt(PH_3)_2$, we evaluated Si−H, Rh−H, and Rh−$SiMe_3$ bond energies, considering the following reactions.

$$HSiMe_3 \rightarrow H + SiMe_3 \quad (1)$$

$$H_2 \rightarrow 2\,H \quad (2)$$

$$RhCl(PH_3)_3 + H_2 \rightarrow cis\text{-}Rh(H)_2Cl(PH_3)_3 \quad (3)$$

$$RhCl(PH_3)_3 + HSiMe_3 \rightarrow cis\text{-}Rh(H)(SiMe_3)Cl(PH_3)_3 \quad (4)$$

As shown in Table 2, these bond energies were calculated with various computational methods. Although the bond energies somewhat fluctuate upon going to MP3 from MP2, the values recover upon going to MP4(SDQ) from MP3. Also, the MP4(SDQ) and CCSD(T) methods yield similar E_a values of eq 4. Hence, we will present our discussion based on bond energies calculated with the MP4(SDQ) method. Apparently, the Rh−H bond is as strong as the Pt−H bond, while the Rh−$SiMe_3$ bond is somewhat stronger than the Pt−$SiMe_3$ bond. Thus, the Si−H oxidative addition to $RhCl(PH_3)_3$ is somewhat more exothermic than that to $Pt(PH_3)_2$. However, the larger E_a value of the Rh reaction system cannot be interpreted in terms of the stronger Rh−$SiMe_3$ bond than the Pt−$SiMe_3$ bond. Moreover, the difference in the E_a value between Pt and Rh reaction systems is much larger than the difference in the ΔE value. These results suggest that the geometry and bonding nature in the transition state contribute to the larger E_a value of the Rh reaction system. One of the reasons is that the geometry of the transition state is congested in the Rh reaction system, as follows: Cl and three PH_3 ligands exist at a position cis to $HSiMe_3$ to give rise to the large steric repulsion with $HSiMe_3$ in the oxidative addition to $RhCl(PH_3)_3$, while two PH_3 ligands cause the steric repulsion with $HSiMe_3$ in the oxidative addition to $Pt(PH_3)_2$. The same discus-

Table 2. Bond Energies (kcal/mol) Related to Oxidative Addition of $HSiMe_3$ to $RhCl(PH_3)_3$

	Rh−H	Rh−SiMe$_3$	Pt−H[a]	Pt−SiMe$_3$[a]
DFT	61.2	44.6		
MP2	61.1	63.7	56.9	56.6
MP3	59.9	52.3	59.4	52.8
MP4(DQ)	62.0	57.7	59.2	53.2
MP4(SDQ)	60.9	59.5	58.8	53.9
CCSD(T)	59.0	55.4		

[a] Ref 13.

sion was presented in the previous theoretical study of oxidative addition of SiH_4 to $MCl(CO)(PH_3)_2$ (M = Rh or Ir).[30]

Ethylene Insertion into the Rh−H Bond. The next step is substitution of PH_3 for ethylene. Since a seven-coordinate complex, $RhClH(SiMe_3)(PH_3)_3(C_2H_4)$, is unusual in 4d transition metal complexes, not associative substitution of PH_3 for ethylene but dissociative substitution would occur, in which PH_3 first dissociates from the Rh center and then ethylene coordinates with the Rh center. $PH_3^{(1)}$, which is at a position trans to $SiMe_3$, easily dissociates from the Rh center because of the strong trans influence of $SiMe_3$, to afford $RhCl(H)(SiMe_3)(PH_3)_2$, **3a**, as shown in Figure 2. Even when $PH_3^{(2)}$ at a position cis to $SiMe_3$ dissociates from the Rh center, $PH_3^{(1)}$ moves to the vacant position cis to $SiMe_3$ with no barrier, to afford **3a** (in other words, ligand movement occurs during the geometry optimization). In **2b**, dissociation of $PH_3^{(1)}$ from the Rh center also induces the movement of Cl to the vacant site at a position cis to $SiMe_3$, to afford **3a**. Dissociation of $PH_3^{(2)}$ from the Rh center also induces the movement of Cl to the vacant site to afford **3b**. This is because the Cl ligand tends to avoid the position trans to $SiMe_3$, the trans influence of which is very strong. The movement of Cl occurs with no barrier, too. Complex **3a** is somewhat more stable than **3b** by 4.2 kcal/mol (DFT/BS-I).

In **3a**, coordination of ethylene with the Rh center affords four isomers of $RhCl(H)(SiMe_3)(PH_3)_2(C_2H_4)$, as shown in Scheme 3. If ethylene approaches the Rh center among Si, P, and Cl to push PH_3 downward, **4a** is formed, in which ethylene takes a position cis to H and $SiMe_3$. If ethylene approaches Rh among Si, P, and Cl to push Cl downward, **4a$_{\#2}$** is formed, in which ethylene is at a position trans to H. If ethylene approaches Rh among H, Si, and P to push H downward, **4a$_{\#3}$** is formed. This structure is very unstable since H and $SiMe_3$ take positions trans to each other. Hence, we excluded this structure from our investigation. If ethylene approaches the vacant site of **3a**, **4a$_{\#4}$** is formed. In **4a$_{\#2}$** and **4a$_{\#4}$**, ethylene is at a position trans to either H or $SiMe_3$. Although **4a$_{\#2}$** and **4a$_{\#4}$** are slightly less stable than **4a** by 3.0 and 2.3 kcal/mol (DFT/BS-II; see Supporting Information Figure S2 for geometries of these complexes), respectively, these structures are significantly unfavorable for the ethylene insertion into the M−$SiMe_3$ and M−H bonds, as follows: In the ethylene insertion into the Rh−$SiMe_3$ bond of **4a$_{\#2}$**, the alkyl ligand is formed at a position trans to H, and in the ethylene insertion into the Rh−H bond of **4a$_{\#4}$**, the alkyl ligand is formed at a position trans to $SiMe_3$. These products are very unstable because of the strong trans influence of H and $SiMe_3$. We will discuss below the unfavorable features of these ethylene insertion reactions in more detail. Thus, **4a$_{\#2}$** and **4a$_{\#4}$** were excluded from investigation of ethylene insertion. In **4a**, we optimized two isomers; ethylene is parallel to the Rh−H bond in one isomer (**4a**) and parallel to the Rh−$SiMe_3$ bond in the other one (**4a′**), as shown in Figure 2. The latter is 4.6 kcal/mol less stable than the former (DFT/BS-II). This is probably because the steric repulsion between ethylene and $SiMe_3$ is smaller in **4a** than in **4a′** (see Figure 2). Actually, the electronic structure of **4a** is almost the same as that of **4a′**; for instance, the Rh atomic population is 45.184 in **4a** and 45.174 in **4a′**, and the electron population of ethylene is 15.907 in **4a** and 15.900 in **4a′**, where the NBO population analysis was adopted.[31]

In **3b**, coordination of ethylene with the Rh center affords five isomers of $RhCl(H)(SiMe_3)(PH_3)_2(C_2H_4)$, **4b**, as shown in Scheme 3. Though **4b$_{\#2}$** is slightly less stable and **4b$_{\#4}$** is slightly more stable than **4b** by 2.9 and 0.4 kcal/mol (DFT/BS-II), respectively, these complexes are unfavorable for ethylene insertion like **4a$_{\#2}$** and **4a$_{\#4}$** (vide supra). Complex **4b$_{\#3}$** is much less stable than the others, since H and $SiMe_3$ take positions trans to each other in this complex. Hence, we investigated ethylene insertion into the Rh−H and Rh−$SiMe_3$ bonds in **4b** and **4c**, in which ethylene takes a position cis to H and $SiMe_3$ (see Figure 2), respectively. The complexes **4a** (0.0), **4a′**(4.6), **4b** (0.5), **4b′** (3.7), **4c** (1.3), and **4c′** (3.6) have similar stabilities, where the numbers in parentheses represent the energy relative to **4a** (kcal/mol; MP4(SDQ)/BS-II).

In **4b**, ethylene is inserted into the Rh−H bond through the transition state **TS$_{4b-5b}$**, to afford $RhCl(CH_2CH_3)(SiMe_3)(PH_3)_2$, **5b**, as shown in Figure 3. Since similar geometry changes are observed in both ethylene insertion reactions of **4a** and **4c**, their geometry changes are omitted here (see Supporting Information Figures S3 and S4 for their geometry changes). In **TS$_{4b-5b}$**, the Rh−C distance (2.173 Å) is similar to that of the product **5b**. On the other hand, the Rh−H distance (1.601 Å) is slightly longer than that of the reactant **4b** by only 0.052 Å, and the C−H distance (1.617 Å) is much longer than the usual C−H bond. From these features, it should be reasonably concluded that the Rh−alkyl bond has been already formed, but the C−H bond formation and Rh−H bond breaking are in progress at the transition state. The same features were observed in the transition state of the ethylene insertion into the Pt−H bond, too.[13,32]

In **5b**, the Rh−H distance is still 1.883 Å and the C−H bond (1.181 Å) is longer than the usual C−H bond (1.10 Å). These features suggest that **5b** involves an agostic interaction between Rh and the C−H bond. To estimate the strength of this agostic interaction, we calculated the isomer of **5b**, in which the ethyl group is rotated around the C−C bond so as to break the agostic interaction (see **5b′** in Figure 3). This isomer is 5.6 kcal/mol less stable than **5b** (DFT(B3LYP)/BS-II), which indicates that the agostic interaction is much weaker than that in $Pt(SiR_3)(CH_2CH_3)(PH_3)$.[13a] Although this

---

[30] Sakaki, S.; Ujino, Y.; Sugimoto, M. *Bull. Chem. Soc. Jpn.* **1996**, *69*, 3047.

[31] Reed, A. E.; Curtis, L. A.; Weinhold, F. *Chem. Rev.* **1988**, *88*, 849, and references therein.

[32] Sakaki, S.; Ogawa, M.; Musashi, Y.; Arai, T. *J. Am. Chem. Soc.* **1994**, *116*, 7258.

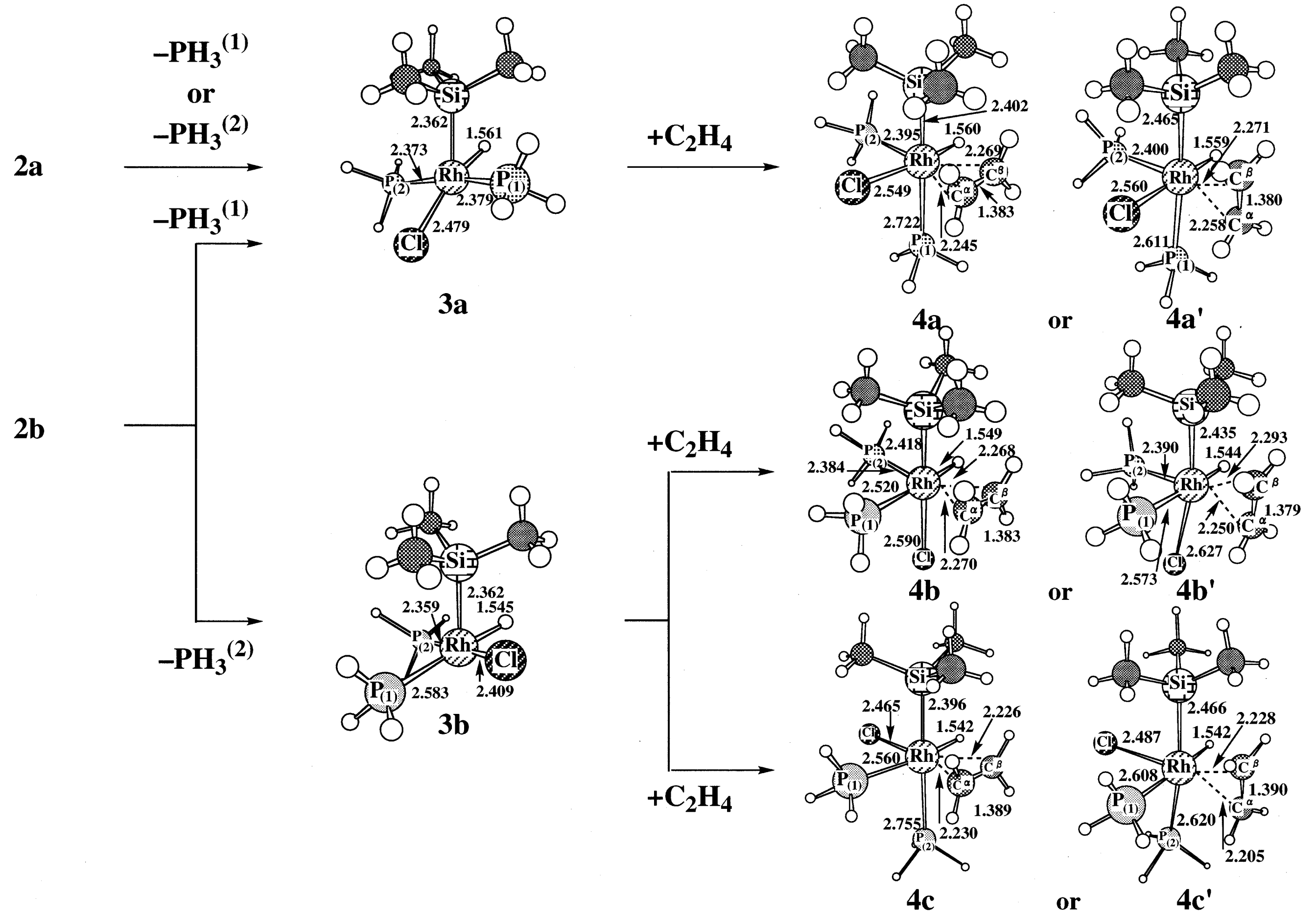

Figure 2. DFT-optimized geometries of coordinatively unsaturated rhodium(III) complexes and rhodium(III) ethylene complexes. Bond lengths in Å and bond angles in deg.

Scheme 3

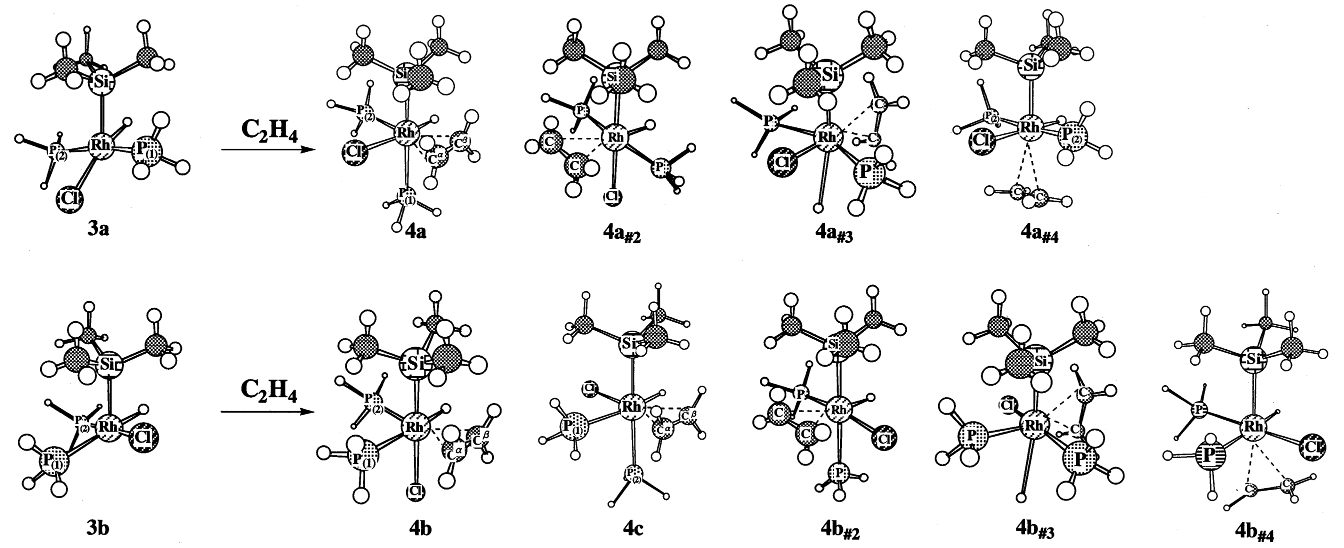

agostic interaction contributes to the stabilization of **5b**, **5b** is not the most stable product because Cl is at a position trans to $SiMe_3$. Thus, **5b** isomerizes to **6b** through $\mathbf{TS_{5b-6b}}$. Then, the ethyl group in **6b** easily rotates to afford the isomer **7b**,[33] which is the same as the product of the insertion reaction starting from **4a**. This complex is the most stable because $SiMe_3$ is at a position trans to an empty site. The agostic interaction between Rh and the C–H bond of the ethyl group is not formed in **7b** probably because the strong trans influence of $SiMe_3$ suppresses the approach of the C–H bond to the Rh center.

Energy changes by the ethylene insertion reaction followed by the isomerization are listed in Table 3. In the ethylene insertion reaction starting from **4a**, the

---

(33) The transition state was not optimized here, since the rotation of the ethyl group would occur very easily.

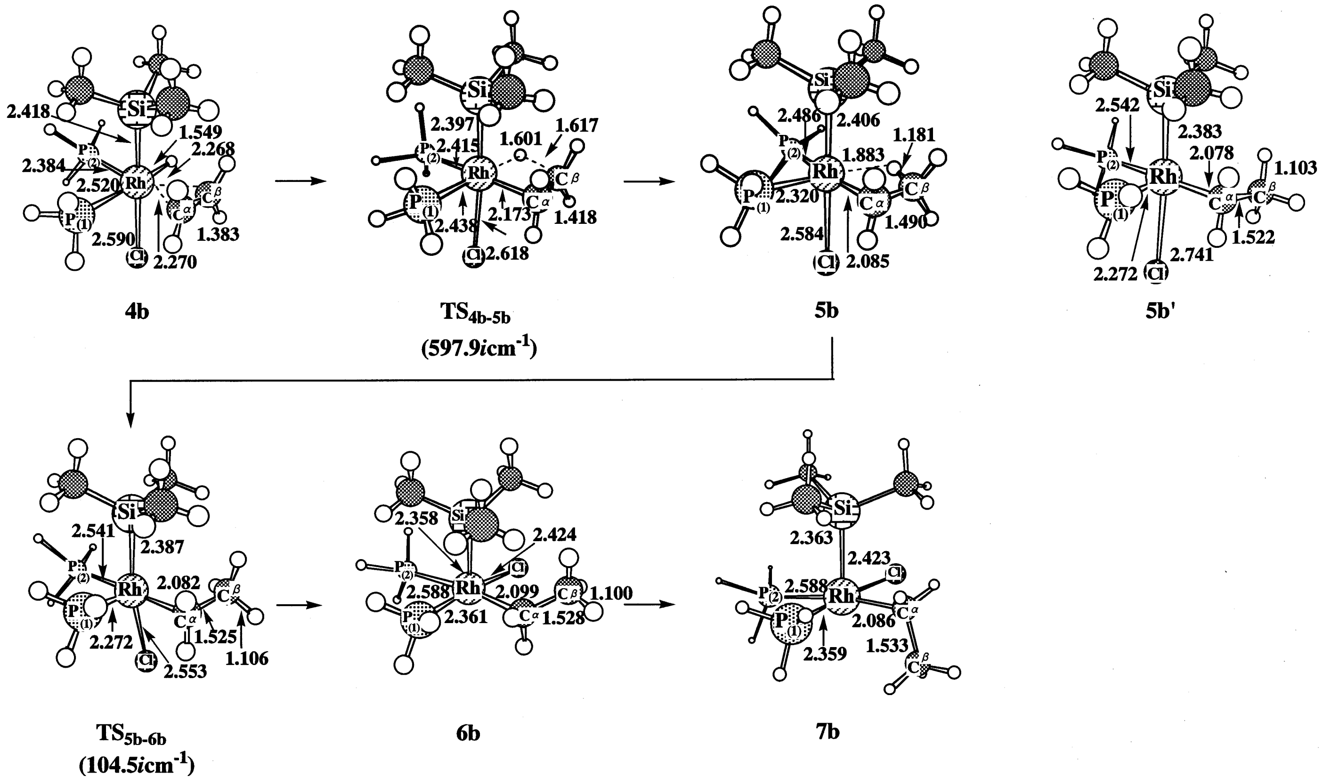

Figure 3. DFT-optimized geometry changes in the ethylene insertion into the Rh−H bond of $RhClH(SiMe_3)(PH_3)_2(C_2H_4)$ **4b**. Bond lengths in Å and bond angles in deg.

Table 3. Energy Changes (kcal/mol) in Ethylene Insertion Reaction into the Rh−H Bond of $RhCl(H)(SiMe_3)(PH_3)_2(C_2H_4)$

	4	TS_4−5	5	TS_5−6	6	7
			4a → 7a			
DFT	0.0	5.9	1.5	7.3 (5.8)[a]	−11.2	−14.1
MP2	0.0	4.4	3.3	16.6 (13.3)	−7.5	−10.8
MP3	0.0	6.1	−1.4	5.3 (6.7)	−12.9	−16.1
MP4(DQ)	0.0	5.8	2.0	12.2 (10.2)	−9.5	−12.7
MP4(SDQ)	0.0	5.9	2.8	13.0 (9.2)	−9.4	−12.5
CCSD(T)				(7.7)		
			4b → 7b			
DFT	(1.9)[b]	0.0	−4.5	0.0 (4.5)	−12.2	−16.0
MP4(SDQ)	(0.5)[b]	−0.6	−4.9	2.1 (7.0)	−8.8	−12.7
			4c → 7c			
DFT	(1.4)[b]	4.8	−2.0	−0.3 (1.7)	−12.1	−15.8
MP4(SDQ)	(1.3)[b]	4.7	−1.1	3.0 (4.1)	−11.0	−14.8

[a] The E_a value (kcal/mol). [b] The relative stabilities (kcal/mol) of **4b** or **4c** to **4a**.

activation barrier (E_a) of the ethylene insertion is calculated to be 5.9 kcal/mol with both the DFT and MP4(SDQ) methods, and the E_a value of the isomerization is calculated to be 5.8 and 9.2 kcal/mol with the DFT and MP4(SDQ) methods, respectively. Since the E_a value of the isomerization is very different between the DFT and MP4(SDQ) methods, we evaluated the E_a value of the isomerization with the CCSD(T) method. The CCSD(T) calculation yields the E_a value of 7.7 kcal/mol, which is about 2 kcal/mol larger than the DFT value and 1.5 kcal/mol smaller than the MP4(SDQ) value. The true E_a value of the isomerization would be intermediate between the DFT and MP4(SDQ) values. In **4b**, ethylene is inserted into the Rh−H bond with nearly no barrier,[34] while the isomerization needs a moderate E_a value, 4.5 kcal/mol by the DFT/BS-II calculation and 7.0 kcal/mol by the MP4(SDQ) calculation. In **4c**, the E_a value of the ethylene insertion is calculated to be 4.8 and 4.7 kcal/mol with the DFT and MP4(SDQ) methods, respectively, and that of the isomerization is calculated to be 1.7 and 4.1 kcal/mol with the DFT and MP4(SDQ) methods, respectively. These computational results show that the ethylene insertion followed by the isomerization more easily takes place in **4b** and **4c** than that in **4a**. Thus, we investigated the Si−C reductive elimination starting from **7b** (=**7a**) and **7c**.

It is worthwhile to investigate the reason that the isomerization most easily occurs in **5c**, since the E_a value for the isomerization is considerably different among these three reaction systems. In the isomerization of **5b**, Cl changes its position, while not Cl but PH_3 changes its position in the isomerizations of **5a** and **5c** (see Supporting Information Figures S3 and S4). Thus, the type of moving ligand is not responsible for the E_a value of the isomerization. An important difference between **5c** and the others is observed in the agostic interaction; in **5c**, the Rh−H distance (1.991 Å) is considerably longer than those of the others (1.890 and 1.883 Å in **5a** and **5b**, respectively). These results clearly indicate that the agostic interaction of **5c** is the weakest, which leads to the smallest E_a value of the isomerization of **5c**.[35]

---

[34] This slightly negative activation barrier would arise from the fact that the transition state structure is slightly different among the DFT/BS-I, DFT/BS-II, and MP4(SDQ)/BS-II optimizations. However, the absolute value of the negative activation barrier is very small. Hence, the discrepancy would be very small, and therefore, it is reasonably concluded that the true activation barrier is very small and the ethylene insertion into the Rh−H bond can be correctly compared with the other elementary processes.

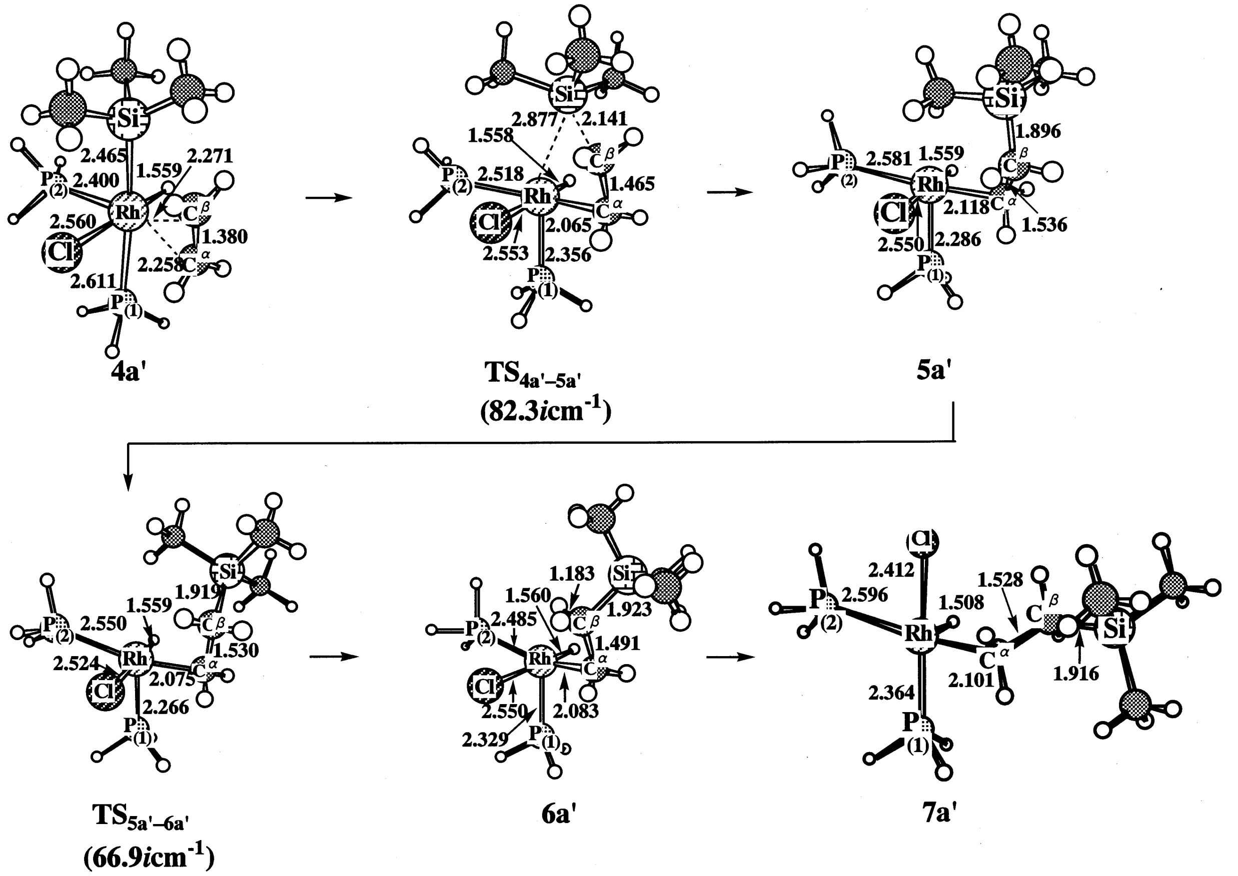

Figure 4. DFT-optimized geometry changes in the ethylene insertion into the Rh−SiMe$_3$ bond of RhClH(SiMe$_3$)(PH$_3$)$_2$-(C$_2$H$_4$), **4a′**. Bond lengths in Å and bond angles in deg.

In summary, the ethylene insertion followed by the isomerization easily occurs with a moderate activation barrier in **4b** and **4c**.

Ethylene Insertion into the Rh−SiMe$_3$ Bond. Geometry changes by the ethylene insertion into the Rh−SiMe$_3$ bond of **4a′** are shown in Figure 4, while those of the ethylene insertion reactions of **4b′** and **4c′** are omitted since their geometry changes are similar to those of **4a′** and also the ethylene insertion reaction of **4b′** needs the largest E_a value in these ethylene insertion reactions, as discussed below (see Supporting Information Figures S5 and S6 for the geometry changes of the insertion reactions of **4b′** and **4c′**). In the transition state **TS$_{4a'-5a'}$**, the Rh−C distance (2.065 Å) is almost the same as that (2.118 Å) of the product **5a′**, whereas the Rh−Si distance (2.877 Å) is about 0.4 Å longer than that (2.465 Å) of the reactant **4a′** and the Si−C distance (2.141 Å) is about 0.25 Å longer than that (1.896 Å) of **5a′**. These features indicate that the Rh−alkyl bond has been almost formed, but the SiMe$_3$ group is still moving from Rh to C$^\beta$ in this TS. In the product **5a′**, one of the methyl groups of SiMe$_3$ occupies the vacant position of Rh, which suggests that the agostic interaction is formed between the C−H bonding orbital of CH$_3$ and the d orbital of Rh. From **5a′**, the isomerization occurs through **TS$_{5a'-6a'}$** to afford **6a′**. Complex **6a′** involves the β-H agostic interaction. Previously reported theoretical work of the Ni- and Pd-catalyzed polymerization of ethylene also showed that the β-H agostic interaction was stronger than the γ-H agostic interaction.[36] Actually, **6a′** is more stable than **5a′** by about 9 kcal/mol (DFT/BS-II). Although we optimized **7a′**, which does not have any agostic interaction, **7a′** is less stable than **6a′** by only 1.3 kcal/mol (DFT/BS-II).

As shown in Table 4, the E_a value of the insertion reaction of **4a′** is calculated to be 13.5 and 16.9 kcal/mol with the DFT and MP4(SDQ) methods, respectively. Then, the isomerization occurs with a very small E_a value; $E_a = 1.2$ and 2.0 kcal/mol by the DFT and MP4(SDQ) calculations, respectively. Since the isomerization easily occurs after the ethylene insertion with a small E_a value, we will focus on the insertion process. DFT and MP4(SDQ) calculations indicate that although **4b′** is slightly more stable than **4a′**, ethylene is inserted into the Rh−SiMe$_3$ bond of **4b′** with a larger E_a value than that of **4a′**, as shown in Table 4. The final product of the insertion reaction of **4b′** is the same as **6a′** (see Supporting Information Figure S5 for geometry changes in the insertion reaction of **4b′** leading to **6a′**). The DFT/BS-II method provides a similar E_a value in both ethylene insertion reactions of **4a′** and **4c′**, while the MP4(SDQ)/BS-II method provides a slightly larger E_a

---

(35) Since PH$_3$ is at a position trans to the agostic interaction in both **5b** and **5c**, the weakest agostic interaction of **5c** is not attributed to the trans-positioned ligand. The Rh−alkyl bond of **5c** is the strongest in these complexes, as shown by its short Rh−C distance, since Cl, whose trans influence is very weak, exists at a position trans to the alkyl group. As a result, the Rh−C$^\alpha$−C$^\beta$ angle is less flexible and more close to the typical angle of sp^3 hybridization than those of the others, which leads to the longer Rh−H distance, and therefore suppresses formation of the Rh−H agostic interaction; actually this angle is 85° in **5c** but about 82° in **5a** and **5b**.

(36) Musaev, D. G.; Foese, R. D. J.; Svensson, M.; Morokuma, K. *J. Am. Chem. Soc.* **1997**, *119*, 367.

Table 4. Energy Changes (kcal/mol) by Ethylene Insertion into the Rh−SiMe$_3$ Bond of RhCl(H)(SiMe$_3$)(PH$_3$)$_2$(C$_2$H$_4$)

	4	**TS$_4$−5**	**5**	**TS$_5$−6**	**6**
		4a′ → 6a′			
DFT	0.0	13.5	5.5	6.7(1.2)[a]	−3.7
MP2	0.0	15.2	13.1	15.2(2.1)	1.9
MP3	0.0	11.0	1.0	3.2(2.2)	−5.8
MP4(DQ)	0.0	15.4	9.0	10.8(1.8)	0.0
MP4(SDQ)	0.0	16.9	11.0	13.1(2.1)	2.2
		4b′ → 6b′			
DFT	(−0.9)[b]	18.9	4.0	5.9(1.9)	4.0
MP4(SDQ)	(−0.5)[b]	24.5			
		4c′ → 6c′			
DFT	(−1.0)[b]	14.3	10.9		
MP4(SDQ)	(−0.9)[b]	19.7	15.6		

[a] The E_a value (kcal/mol). [b] The relative stabilities (kcal/mol) of **4b′** or **4c′** to **4a′**.

value in the reaction of **4c′** than that in **4a′**. From these results, it should be concluded that ethylene is easily inserted into the Rh−SiMe$_3$ bond in **4a′** and **4c′** to yield **6a′** and **6c′**, respectively, but the ethylene insertion reaction is difficult in **4b′**.

Here, it should be noted that ethylene can be inserted into the Rh−SiMe$_3$ bond with a much smaller E_a value than that into the Pt−SiR$_3$ bond, which needs a significantly large activation barrier of 40−60 kcal/mol.[13] This difference is of considerable importance, since the very large E_a value of the ethylene insertion into the Pt−SiR$_3$ bond leads to the fact that the Pt-catalyzed hydrosilylation cannot proceed through the modified Chalk−Harrod mechanism. In the Rh reaction system, on the other hand, this mechanism is not unfavorable, because of the moderate E_a value of the ethylene insertion into the Rh−SiMe$_3$ bond. The reason for this difference will be discussed below in detail.

Si−C Reductive Elimination Reaction of RhCl(CH$_3$)(SiMe$_3$)(PH$_3$)$_2$L (L = PH$_3$ or C$_2$H$_4$). After ethylene is inserted into the Rh−H bond, Si−C reductive elimination must take place to complete the catalytic cycle. As described above, we will investigate the Si−C reductive elimination starting from **7b** and **7c**. Either PH$_3$ or ethylene easily coordinates with the Rh center to form RhCl(C$_2$H$_5$)(SiMe$_3$)(PH$_3$)$_2$L, since **7b** and **7c** are coordinatively unsaturated. Here, we adopted a model complex, RhCl(CH$_3$)(SiMe$_3$)(PH$_3$)$_2$L (**8b** for L = C$_2$H$_4$ and **8b′** for L = PH$_3$), to save CPU time. This model is not unreasonable because the agostic interaction is not involved in **7b** and **7c**. In **8b′**, PH$_3$ eliminates from the Rh center during optimization of the transition state, and we failed to optimize the transition state. Since ethylene coordination with the Pt(II) center facilitates the Si−C and C−H reductive eliminations of Pt(II) complexes compared to phosphine coordination,[13] we stopped further investigation of the Si−C reductive elimination of **8b′**. In **8b**, the Si−C reductive elimination occurs through the transition state **TS$_{8b-9}$** to afford RhCl(PH$_3$)$_2$(C$_2$H$_4$) **9**, as shown in Figure 5. In **TS$_{8b-9}$**, the Si−C distance is 2.029 Å, which is only 0.1 Å longer than that of tetramethylsilane, while the Rh−C distance is considerably longer than that of the reactant **8b**. Although the Rh−Si distance does not lengthen very much, the SiMe$_3$ group moves considerably toward the CH$_3$ group. All these geometrical features indicate that the Si−C bond is almost formed without complete breaking of the Rh−SiMe$_3$ bond; in other words, the well-known hypervalency of the Si element plays an important role in this transition state, which facilitates the reaction. A similar contribution of hypervalency was reported in the reductive elimination of Pd(EH$_3$)(η^3-C$_3$H$_5$)(PH$_3$) (E = Si, Ge, or Sn).[37] Interestingly, orientation of ethylene changes and the Rh−ethylene distance becomes much shorter upon going to **TS$_{8b-9}$** from **8b**. These geometrical changes are related to the acceleration of Si−C reductive elimination by ethylene, as follows: Since the electron population of the Rh d orbital increases in the Si−C reductive elimination, the π acceptor ligand stabilizes the transition state and the product through the π-back-donation interaction. Actually, the C═C double bond of ethylene is on the plane that consists of Rh, PH$_3$(2), Si, and CH$_3$ so as to overlap well the π* orbital of ethylene with the d orbital of Rh that is destabilized in energy by PH$_3$$^{(2)}$, SiMe$_3$, and CH$_3$ groups in **TS$_{8b-9}$**. Also, the electron population of ethylene increases and the C═C distance lengthens upon going to **TS$_{8b-9}$** from **8b**; the electron population of ethylene is 15.997*e* in **8** and 16.045*e* in **TS$_{8b-9}$**;[38] see Figure 5 for the C═C distance. Thus, it should be concluded that ethylene accelerates the reductive elimination through the π-back-donation interaction.

Complex **7c** undergoes ethylene coordination to afford **8c** (see Supporting Information Figure S4 for **7c**). The Si−C reductive elimination of **8c** also occurs with geometry changes similar to those of **8b**, while its geometry changes are omitted here since the activation barrier is somewhat larger than that of the reductive elimination of **8c** (see below).

The activation energy and reaction energy are listed in Table 5. The E_a value of the Si−C reductive elimination of **8b** is calculated to be 27.4 kcal/mol with the DFT method and 28.8 kcal/mol with the MP4(SDQ) method. The Si−C reductive elimination of **8c** occurs with a somewhat larger activation barrier of 31.2 kcal/mol than that of the reductive elimination of **8b** (DFT/BS-II). It should be noted that these E_a values are much larger than that of the Si−C reductive elimination of Pt(SiMe$_3$)(CH$_3$)(PH$_3$)(C$_2$H$_4$).[13]

C−H Reductive Elimination of RhCl(H)(CH$_2$CH$_2$SiMe$_3$)(PH$_3$)$_2$L (L = PH$_3$ or C$_2$H$_4$). The C−H reductive elimination must occur after the ethylene insertion into the Rh−SiMe$_3$ bond to complete the catalytic cycle. We investigate the C−H reductive elimination starting from RhCl(H)(CH$_2$CH$_2$SiMe$_3$)(PH$_3$)$_2$ **6a′** and **6c′**, which are products of the insertion reactions of **4a′** and **4c′**, respectively. Either ethylene or PH$_3$ coordinates with the Rh center in **6a′** and **6c′** to afford RhCl(H)(CH$_2$CH$_2$SiMe$_3$)(PH$_3$)$_2$L (L = PH$_3$ or C$_2$H$_4$), since the agostic interaction is weaker than the coordinate bonds of phosphine and ethylene. Here, we adopted a model complex, RhCl(H)(CH$_3$)(PH$_3$)$_2$L (**10a** for L = C$_2$H$_4$ and **10a′** for L = PH$_3$), for **6a′** and **6c′**. This is not unreasonable since the coordination of PH$_3$ and ethylene breaks the agostic interaction of **6a′** and

---

(37) Biswas, B.; Sugimoto, M.; Sakaki, S. *Organometallics* **1999**, *18*, 4015.

(38) In the product **9**, the electron population of ethylene is 15.937*e*, which is smaller than that of **TS$_{8b-9}$**. This is probably because the electron donation of ethylene to Rh becomes strong in the product (note that the π orbital of ethylene overlaps well with the empty d$_\sigma$ orbital of Rh in the product).

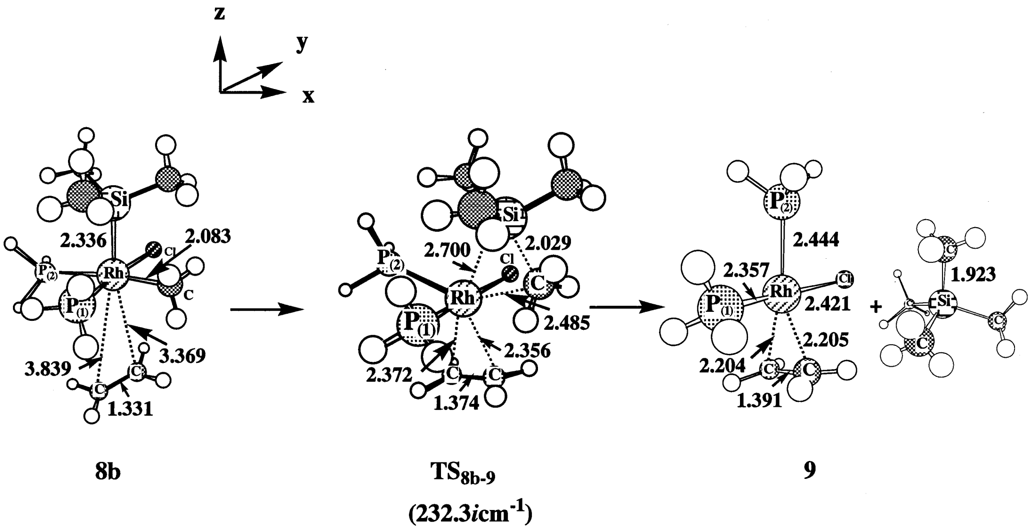

Figure 5. DFT-optimized geometry changes in the Si−C reductive elimination from $RhCl(SiMe_3)(CH_3)(PH_3)_2(C_2H_4)$, **8a**. Bond lengths in Å and bond angles in deg.

Table 5. Activation Barrier (E_a)[a] and Reaction Energy (ΔE)[b] of C−H and Si−C Reductive Eliminations (kcal/mol)

	E_a	ΔE
	Si−C Reductive Elimination of $RhCl(CH_3)(SiMe_3)(PH_3)_2L$	
	8b → **9** (L = C_2H_4)	
DFT	27.4	−10.3
MP4(SDQ)	28.8	
	8c → **9** (L = C_2H_4)	
DFT	31.2	−14.6
	C−H Reductive Elimination	
	10a → **9** (L = C_2H_4)	
DFT	9.9	−24.5
	10c → **9** (L = C_2H_4)	
DFT	10.2	−22.3
	10a′ → **1** (L = PH_3)	
DFT	16.7	−18.8
	10c′ → **1** (L = PH_3)	
DFT	16.7	−18.0

[a] The energy difference between the transition state and the reactant. [b] The energy difference between the product and the reactant.

6c′. When L is C_2H_4, the C−H reductive elimination proceeds through the transition state $\mathbf{TS_{10a-9}}$ to afford $RhCl(PH_3)_2(C_2H_4)$, **9**, as shown in Figure 6. In $\mathbf{TS_{10a-9}}$, the C−H distance is 1.569 Å, the Rh−H distance is 1.585 Å, and the Rh−CH_3 distance is 2.238 Å. These features indicate that the Rh−H and Rh−CH_3 bonds are still maintained, but the C−H bond is not completely formed yet in this TS; in other words, this TS is reactant-like. When L is PH_3, the reductive elimination occurs through the transition state $\mathbf{TS_{10a'-1}}$ to afford $RhCl(PH_3)_3$, **1** (see Figure 6). As shown in Figure 6, $\mathbf{TS_{10a'-1}}$ resembles well $\mathbf{TS_{10a-9}}$.

The activation barrier (E_a) and the reaction energy (ΔE) are listed in Table 5. Since the DFT method yields E_a and ΔE values similar to the MP4(SDQ) method in the Si−C reductive elimination, we adopted the DFT method in the C−H reductive elimination, too. Apparently, the C−H reductive eliminations of **10a** and **10c** need a similar E_a value of about 10 kcal/mol. Also, the E_a values for $\mathbf{TS_{10a-9}}$ and $\mathbf{TS_{10c-9}}$ are much smaller than those for $\mathbf{TS_{10a'-1}}$ and $\mathbf{TS_{10c'-1}}$ like the C−H reductive elimination of the Pt system, in which ethylene coordination with the Pt(II) center decreases the E_a value of the C−H reductive elimination.[13] We omitted here the discussion of the reason that ethylene coordination accelerates the C−H reductive elimination compared to phosphine coordination, since it was discussed above and previously.[13]

Energy Changes along the Whole Catalytic Cycle. Now, we have completed all the preparations for the discussion of energy changes along the whole catalytic cycle. Since ethylene is more easily inserted into the Rh−H bond in **4b** and **4c** than in **4a**, we examined the energy changes along **1** → **2a** → **3b** → **4b** → **5b** → **7b** → **8b** → **9** (course A) and **1** → **2a** → **3b** → **4c** → **5c** → **7c** → **8c** → **9** (course B) in the Chalk−Harrod mechanism. In the modified Chalk−Harrod mechanism, ethylene is more easily inserted into the Rh−$SiMe_3$ bond in **4a′** and **4c′** than that in **4b′**. Thus, we examined the energy changes along **1** → **2a** → **3a** → **4a′** → **5a′** → **6a′** → **10a** → **9** (course C) and **1** → **2b** → **3b** → **4c′** → **5c′** → **6c′** → **10b** → **9** (course D). Energy changes of course A and course C are displayed in Figure 7, where values without parenthesis and in parenthesis are calculated with the DFT/BS-II and MP4(SDQ)/BS-II methods, respectively. Apparently, the rate-determining step of the Chalk−Harrod mechanism is the Si−C reductive elimination, the activation energy of which is 27.4 kcal/mol in course A (DFT/BS-II). This barrier is 31.2 kcal/mol in course B (DFT/BS-II). In the modified Chalk−Harrod mechanism, on the other hand, the rate-determining step is the oxidative addition of H−$SiMe_3$ (E_a = 15.7 kcal/mol) at the DFT/BS-II level and the ethylene insertion into the Rh−$SiMe_3$ bond at the MP4(SDQ)/BS-II level, the activation barrier of which is 16.9 kcal/mol in course C and 19.7 kcal/mol in course D. In both cases, however, the E_a value is much smaller than that of the rate-determining step of the Chalk−Harrod mechanism. Thus, it should be reasonably concluded that the modified Chalk−Harrod mechanism is more favorable than the Chalk−Harrod mechanism in the Rh-catalyzed hydrosilyaltion of ethylene, unlike the Pt-catalyzed hydrosilylation of ethylene, which takes place through the Chalk−Harrod mechanism.[13]

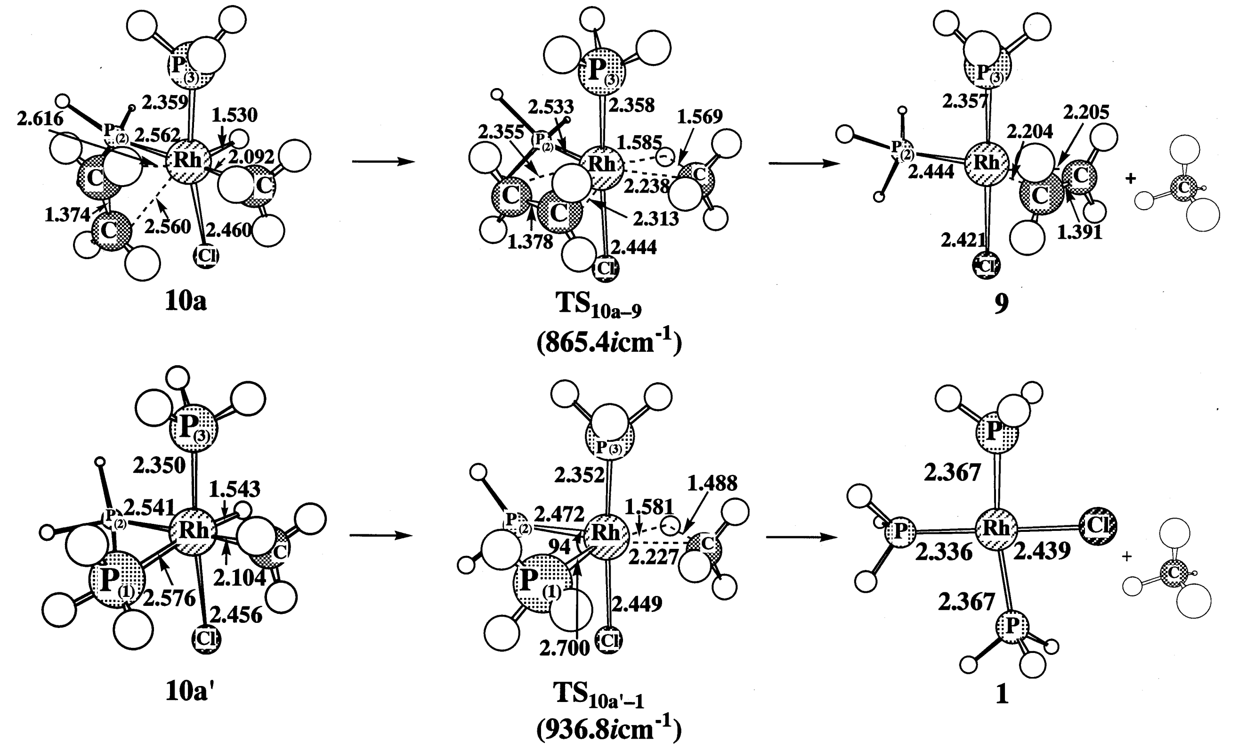

Figure 6. DFT-optimized geometry changes in the C−H reductive elimination from RhCl(H)(CH$_3$)(PH$_3$)$_2$L (L = C$_2$H$_4$ for **10a** and PH$_3$ for **10a′**). Bond lengths in Å and bond angles in deg.

To complete a catalytic cylcle, the oxidative addition of HSiMe$_3$ must occur with RhCl(PH$_3$)$_2$(C$_2$H$_4$), **9**. Finally, we theoretically investigated this oxidative addition reaction. This oxidative addition proceeds through the transition state which is similar to those of the oxidative addition of HSiMe$_3$ to RhCl(PH$_3$)$_3$, **TS$_{1-2a}$** and **TS$_{1-2b}$**, as shown in Figure 8. The activation barrier is calculated to be 19.2 kcal/mol when **4b** is produced and 12.5 kcal/mol when **4a** is produced (DFT/BS-II). These values are not very much different from those of the oxidative addition to RhCl(PH$_3$)$_3$. Since the activation barrier leading to **4a** is smaller than those of the rate-determining steps of the Chalk−Harrod and modified Chalk−Harrod mechanisms, the conclusion of the reaction mechanism does not change by taking this oxidative addition into consideration. Remember that **4b** is not involved in the courses C and D.

Formation of Vinylsilane. The other issue to be investigated is formation of vinylsilane, since formation of vinylsilane as a byproduct is considered one of the important pieces of evidence for the modified Chalk−Harrod mechanism.[6−8,10] The β-H abstraction by the Rh center was investigated in **6a′**, as shown in Figure 9. In the transition state **TS$_{6a'-12a}$**, the Rh−H and C−H distances are 1.590 and 1.662 Å, respectively, which indicates that the Rh−H bond is almost formed and the C$^{\beta}$−H bond is almost broken. In the product, *cis*-$\overline{\text{RhCl(H)}_2\text{(PH}_3)_2\text{(CH}_2}$=CH−SiMe$_3$) **12a**, vinylsilane coordinates with the Rh center. The Rh−C distances of 2.288 and 2.256 Å are in the range of normal coordinate bond distances. In the β-H abstraction of **6b′**, essentially the same geometry changes are observed (see Supporting Information Figure S8 for geometry changes in the β-H abstraction of **6b′**).

The E_a value was calculated to be 6.3 kcal/mol for **6a′** and 3.6 kcal/mol for **6b′** with the DFT/BS-II method (see Table 6).[39] The reverse insertion of vinylsilane into the Rh−H bond more easily occurs with E_a values of 2.5 and 6.0 kcal/mol to yield **6a′** and **6b′**, respectively. From these results, the following conclusions are presented: (1) the β-H abstraction by the Rh center rapidly occurs to afford vinylsilane as a byproduct in this catalytic reaction when ethylene exists enough to substitute vinylsilane, and (2) although the β-H abstraction easily occurs with a smaller E_a value than that of the C−H reductive elimination, the insertion of vinylsilane into the Rh−H bond much more easily occurs than the β-H abstraction, and therefore, the hydrosilylation takes place easily. It is clearly concluded that the hydrosilylation takes place through the modified Chalk−Harrod mechanism where vinylsilane is produced as a byproduct in the early stage of the reaction in which alkene exists in excess. Also, we wish to propose that the ethylene concentration should not be kept too high to efficiently perform the hydrosilylation; if not, vinylsilane is formed.

After formation of $\overline{\text{RhCl(H)}_2\text{(PH}_3)_2\text{(CH}_2}$=CHSiMe$_3$) (**12a** and **12a′**), the reductive elimination of H$_2$ must occur to regenerate the Rh(I) species. This reductive elimination of **12a** takes place with a moderate activation barrier of 11.9 kcal/mol (DFT/BS-II), where the transition state is given in Figure 10.

Comparison of Ethylene Insertion Reaction between Pt and Rh. It is of considerable importance to clarify the reason that the modified Chalk−Harrod mechanism is favorable in the Rh catalyst but the

---

[39] Since both DFT and MP4(SDQ) methods provide similar E_a values in the insertion reaction, we did not calculate the E_a value with the MP4(SDQ) and CCSD(T) methods.

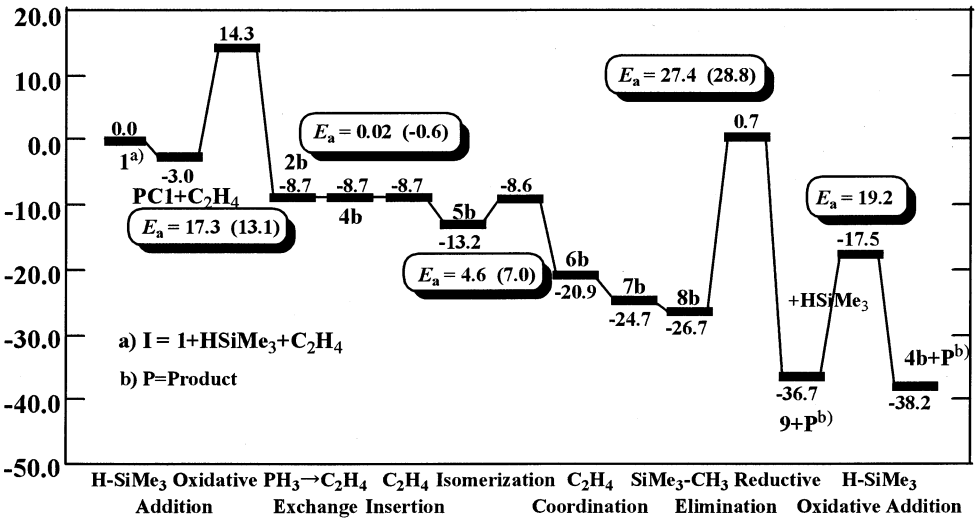

(A) Chalk-Harrod mechanim including the ethylene insertion into Rh-H bond.

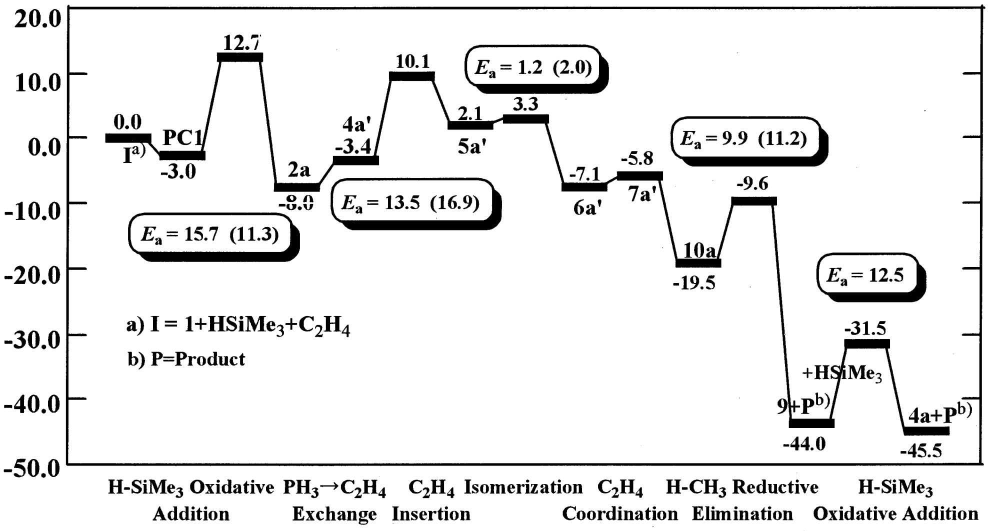

(B) Modified Chalk-Harrod mechanim including the ethylene insertion into Rh-$SiMe_3$ bond

Figure 7. Energy changes along the catalytic cycle of $RhCl(PH_3)_3$-catalyzed hydrosilylation of ethylene in the Chalk–Harrod mechanism (upper) and modified Chalk–Harrod mechanism (lower). Values without parentheses and with parentheses are energy changes calculated by DFT and MP4(SDQ) methods, respectively.

Chalk–Harrod mechanism is favorable in the Pt catalyst. As discussed above, ethylene is more easily inserted into the Rh–H bond than into the Rh–$SiMe_3$ bond. Nevertheless, Rh-catalyzed hydrosilylation proceeds not through the Chalk–Harrod mechanism but through the modified Chalk–Harrod mechanism. There are two reasons: (1) the Si–C reductive elimination that is involved in the Chalk–Harrod mechanism requires a very large activation barrier, and (2) ethylene is inserted into the Rh–$SiMe_3$ bond with a moderate E_a value, which is smaller than the E_a value of the Si–C reductive elimination. In the Pt-catalyzed hydrosilylation, on the other hand, the ethylene insertion into the Pt–SiR_3 bond requires a very large activation energy. This barrier is much larger than the barrier of the Si–C reductive elimination.[13] Thus, Pt-catalyzed hydrosilylation occurs through the Chalk–Harrod mechanism.

The above results suggest that the difference in the ethylene insertion reaction between Rh and Pt catalysts is one of the important reasons for the different reaction mechanism between these catalysts. Since the metal–alkyl bond is almost formed in the transition state of the ethylene insertion reaction, as has been discussed above, the ligand at a position trans to ethylene significantly contributes to the stability of the transition state. In the modified Chalk–Harrod mechanism of Pt-catalyzed hydrosilylation of ethylene,[13] the Pt–alkyl bond is formed at a position trans to H(hydride) (see Figure 4 of ref 13a). This situation is significantly unfavorable because two strong ligands, H and alkyl, take positions trans to each other. In the ethylene insertion reaction of $RhCl(H)(SiMe_3)(PH_3)_2(C_2H_4)$, **4a′**, on the other hand, the Rh–alkyl bond is formed at a position trans to PH_3. This is favorable since the trans influence of PH_3 is much weaker than that of H. Even

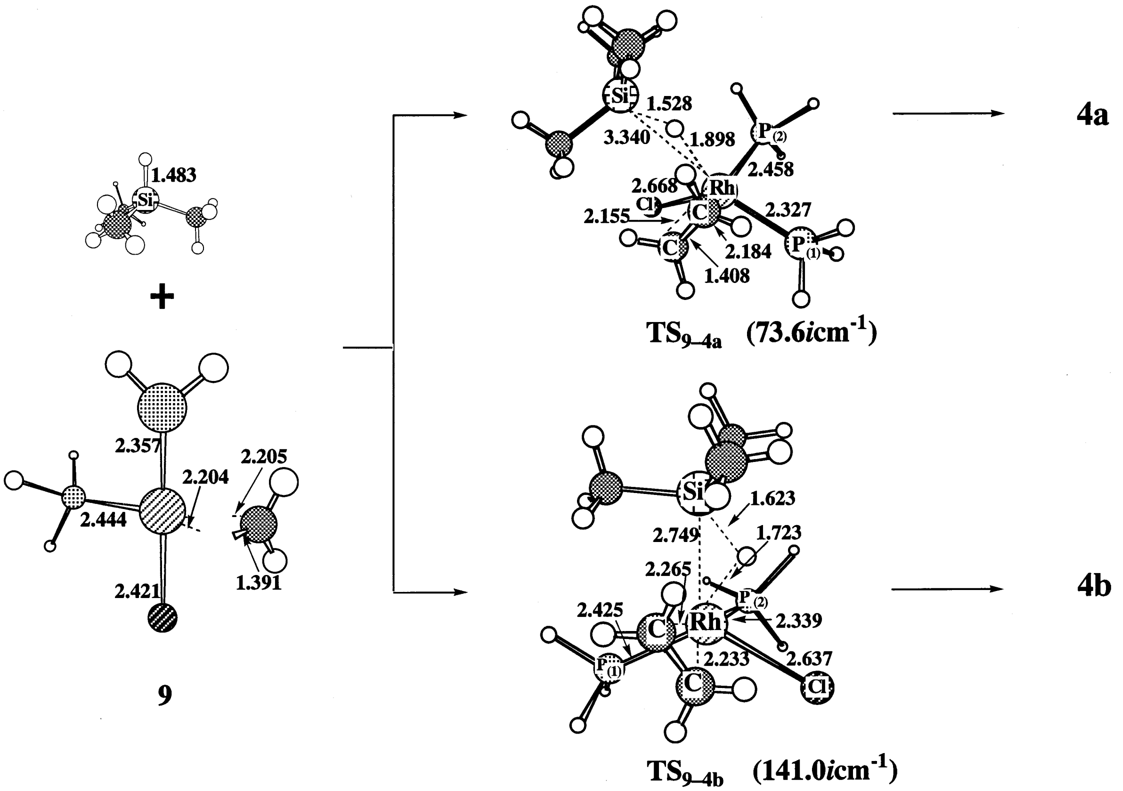

Figure 8. DFT-optimized geometry changes in the Si–H oxidative addition of $SiHMe_3$ to $RhCl(PH_3)_2(C_2H_4)$. Bond lengths in Å and bond angles in deg.

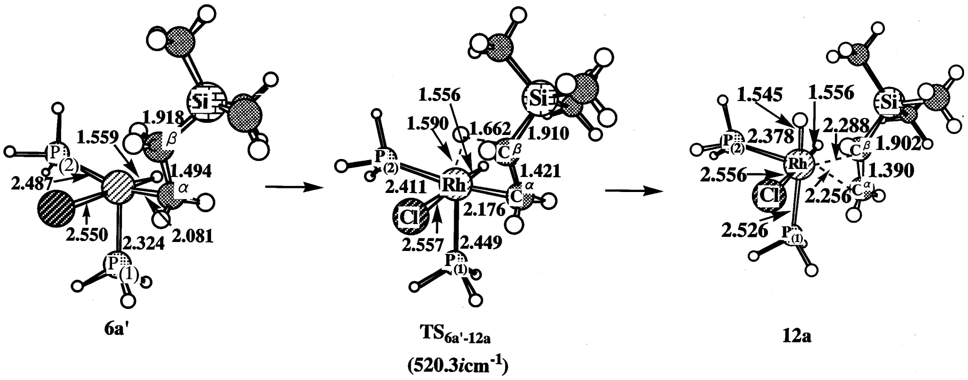

Figure 9. DFT-optimized geometry changes in the β-H abstraction reaction of $RhCl(H)(CH_2CH_2SiMe_3)(PH_3)_2$, **6a′**. Bond lengths in Å and bond angles in deg.

Table 6. Activation Barrier (E_a)[a] and Reaction Energy (ΔE)[b] of β-H Abstraction of $RhCl(H)(CH_2CH_2SiMe_3)(PH_3)_2$ (kcal/mol)

	E_a	ΔE
6a′	6.3	4.6
6b′	3.6	−1.5

[a] DFT(B3LYP)/BS-II.

in the Pt(II) complex, ethylene is easily inserted into the Pt–SiR_3 bond with a moderate E_a value when ethylene is at a position trans to PH_3.[13b,c] In RhCl(H)-$(SiMe_3)(PH_3)_2(C_2H_4)$, we calculated the assumed structure of the transition state in which positions of H and PH_3 were exchanged with each other with the geometry of the other moiety fixed to be the same as that of $\mathbf{TS_{4a'-5a'}}$.[40] As shown in Scheme 4, this assumed structure is much more unstable than $\mathbf{TS_{4a'-5a'}}$ by 49.6 kcal/mol (DFT/BS-II). These results lead us to the following conclusions: (1) the E_a value of the ethylene insertion reaction significantly depends on the ligand at a position trans to ethylene, and (2) the important difference between the Pt and Rh catalysts arises from the fact that ethylene can take a position trans to PH_3 in Rh(III) complexes but must take a position trans to H in Pt(II) complexes.

We will investigate what factor is responsible for this difference in geometry. We can easily find the factor by observing the geometry of the ethylene complexes. Because of the d^6 electron configuration of Rh(III), the Rh(III) complex takes in general a six-coordinate structure such as $RhCl(H)(SiMe_3)(PH_3)_2(C_2H_4)$, in which ethylene can exist at a position trans to PH_3, in other words, a position cis to $SiMe_3$ and H(hydride). On the

---

[40] We tried to optimize the transition state of ethylene insertion starting from $RhCl(H)(SiMe_3)(C_2H_4)(PH_3)_2$, in which ethylene takes a position trans to $SiMe_3$. However, we failed to optimized it. Thus, we calculated the assumed transition state structure ($\mathbf{TS_{assumed}}$ in Scheme 4) which was obtained from $\mathbf{TS_{4a'-5a'}}$ by exchanging ethylene and PH_3.

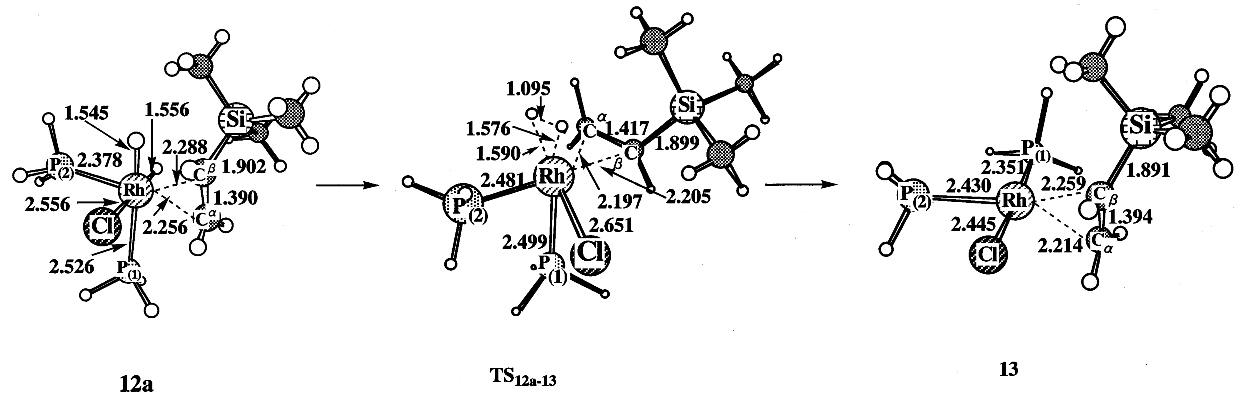

Figure 10. DFT-optimized transition state of H−H reductive elimination from $\overline{\mathrm{RhCl(H)_2(PH_3)_2(CH_2{=}C}}\mathrm{HSiMe_3)}$. Bond lengths in Å and bond angles in deg.

Scheme 4

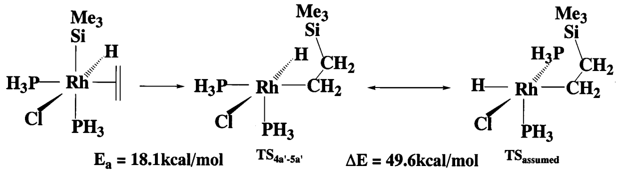

other hand, the Pt(II) complex takes in general a four-coordinate planar structure such as *cis*-PtH(SiMe$_3$)(PH$_3$)(C$_2$H$_4$) because of the d^8 electron configuration of Pt(II). In the four-coordinate structure, ethylene must take a position trans to H in PtH(SiMe$_3$)(PH$_3$)(C$_2$H$_4$) to cause the ethylene insertion into the Pt−SiMe$_3$ bond, since the Si−H oxidative addition of hydrosilane yields a platinum(II) hydride silyl complex with a cis form (see Figure 4 of ref 13a). Thus, it should be clearly concluded that the important difference between Pt and Rh arises from the different d electron number. From this conclusion, we wish to propose that the modified Chalk−Harrod mechanism is more favorable than the Chalk−Harrod mechanism when a catalyst takes a d^6 electron configuration.

Comparison of Si−C Reductive Elimination between Pt and Rh. The other important difference between Rh and Pt catalysts is observed in the Si−C reductive elimination. In Pt-catalyzed hydrosilylation, the Si−C reductive elimination occurs with a moderate activation barrier (6.8 kcal/mol; MP4(SDQ)), which is similar to that of the C−H reductive elimination. In the Rh-catalyzed hydrosilylation, on the other hand, the activation barrier of the Si−C reductive elimination (27−31 kcal/mol; DFT/BS-II) is much larger than that of the C−H reductive elimination (about 10 kcal/mol). Since the activation barrier of the Si−C reductive elimination is much larger than that of the ethylene insertion into the Rh−SiMe$_3$ bond, the modified Chalk−Harrod mechanism is more favorable than the Chalk−Harrod mechanism in the Rh reaction system. Thus, it is of importance to clarify the reason that the Si−C reductive elimination needs a considerably large activation barrier. This is easily interpreted in terms of valence orbitals of H(hydride), CH$_3$, and SiMe$_3$;[41] since the sp^3 valence orbitals of CH$_3$ and SiMe$_3$ are directional, the direction of SiMe$_3$ must change toward CH$_3$ and that of CH$_3$ also must change toward SiMe$_3$ in the Si−C reductive elimination. In the C−H reductive elimination; on the other hand, only CH$_3$ must change its direction toward H (note that H(hydride) has a spherical 1s valence orbital). As a result, the Si−C reductive elimination needs a larger activation barrier than does C−H reductive elimination. A similar explanation has been presented in C−H and C−C oxidative additions[42−44] and insertions of ethylene and carbon dioxide into the metal−hydride, metal−alkyl, and metal−silyl bonds.[13,32,45]

The remaining issue to be investigated is the reason that the Si−C reductive elimination can occur with an activation barrier similar to that of the C−H reductive elimination in the Pt reaction system. Since Pt−H and Pt−SiMe$_3$ bond energies are similar to Rh−H and Rh−SiMe$_3$ bond energies (see Table 2), these bond energies are not responsible for the reason. At this moment, the reason for the moderate activation barrier of the Si−C reductive elimination in the Pt reaction system is ambiguous, and we need further detailed investigation about this issue in the future.

Conclusions

In this work, all the elementary steps of the Chalk−Harrod and modified Chalk−Harrod mechanisms were investigated, to clarify the reaction mechanism of RhCl(PH$_3$)$_2$-catalyzed hydrosilylation of ethylene. Important results are summarized, as follows: (1) The rate-determining step in the Chalk−Harrod mechanism is Si−C reductive elimination. (2) The rate-determining step of the modified Chalk−Harrod mechanism is ethylene insertion into the Rh−SiMe$_3$ bond at the MP4(SDQ)/BS-II level and oxidative addition of H−SiMe$_3$ at the DFT/BS-II level. (3) Since the Si−C reductive elimination needs a much larger activation barrier than the oxidative addition of H−SiMe$_3$ and ethylene insertion into the Rh−SiMe$_3$ bond, the modified Chalk−Harrod mechanism is more favorable than the Chalk−Harrod mechanism in the Rh-catalyzed hydrosilylation

---

[41] Sakaki, S.; Ieki, M. *J. Am. Chem. Soc.* **1993**, *115*, 2375.

[42] Saillard, J.-Y.; Hoffmann, R. *J. Am. Chem. Soc.* **1984**, *108*, 6587.

[43] (a) Blomberg, M. R. A.; Brandemark, U.; Siegbahn, P. E. M. *J. Am. Chem. Soc.* **1983**, *105*, 5557. (b) Blomberg, M. R. A.; Siegbahn, P. E. M.; Nagashima, U.; Wennerberg, J. *J. Am. Chem. Soc.* **1991**, *113*, 424.

[44] Low, J. J.; Goddard, W. A. *Organometallics* **1986**, *5*, 609. (b) Low, J. J.; Goddard, W. A. *J. Am. Chem. Soc.* **1986**, *108*, 6115.

[45] (a) Sakaki, S.; Musashi, Y. *Inorg. Chem.* **1995**, *34*, 1914. (b) Sugimoto, M.; Yamasaki, I.; Mizoe, N.; Anzai, M.; Sakaki, S. *Theor. Chem. Acc.* **1999**, *102*, 377.

of ethylene, unlike the Pt-catalyzed hydrosilylation of alkene, which takes place through the Chalk−Harrod mechanism.

The difference between Rh and Pt catalysts arises from the fact that the Rh(III) ion has a d^6 electron configuration but the Pt(II) ion has a d^8 electron configuration, as follows: The Rh(III) complex takes a six-coordinate structure such as $RhCl(H)(SiMe_3)(PH_3)_2(C_2H_4)$ because of its d^6 electron configuration. In this complex, ethylene can take a position cis to H and $SiMe_3$, i.e., trans to PH_3, and therefore, ethylene insertion into the Rh−$SiMe_3$ bond leads to formation of the Rh-alkyl bond at the position trans to PH_3. Since this structure does not suffer from the strong trans influence of the H ligand, the ethylene insertion occurs with a moderate activation barrier. On the other hand, the Pt(II) complex takes a four-coordinate structure because of its d^8 electron configuration. As a result, ethylene must take a position trans to H or $SiMe_3$, and therefore, ethylene insertion into the Pt−$SiMe_3$ bond leads to formation of the Pt−alkyl bond at the position trans to the H ligand. Because of the strong trans influence of H, this structure is very unstable, which results in the large E_a value. The other difference is observed in the Si−C reductive elimination, as follows: the Si−C reductive elimination is much more difficult than the C−H reductive elimination in the Rh system. This difference is interpreted in terms of the directional sp^3 valence orbitals of $SiMe_3$ and CH_3. From these differences, the modified Chalk−Harrod mechanism is more favorable than the Chalk−Harrod mechanism in the Rh-catalyzed hydrosilylation of ethylene. It is also suggested that the hydrosilylation occurs through the modified Chalk−Harrod mechanism when the active species takes a d^6 electron configuration.

We expect in general that reactions of transition metal complexes significantly depend on the d electron number. However, such an example has been scarcely found. In this work, it is clearly shown how the reaction mechanism depends on the d electron number of the transition metal element.

Acknowledgment. This work is financially supported in part by a Grant-in-Aid for Scientific Research on the Priority Areas “Molecular Physical Chemistry (No. 403)” and “Exploitation of Multi-Element Cyclic Molecules (No. 412)” from the Ministry of Education, Science, Sports, and Culture of Japan.

Supporting Information Available: Hartree−Fock optimized geometries and MP2-calculated relative energies of three isomers of $RhClH(SiMe_3)(PMe_3)_3$, and geometry changes and energy changes in ethylene insertion into the Rh−H bond of **4a** and **4c**, ethylene insertion into the Rh−$SiMe_3$ bond of **4b′** and **4c′**, C−H reductive elimination of **10b** and **10b′**, *β*-H abstraction reaction of $RhClH(CH_2CH_2SiMe_3)(PH_3)_2$, reductive elimination of H_2 from $RhCl(H)_2(CH_2{=}CHSiMe_3)(PH_3)_2$, and eigenvector in the imaginary frequency of transition states. This material is available free of charge via the Internet at http://pubs.acs.org.

OM020239J